

## REFERENCES

- [1] Braasch, M. (1994–1995)  
Isolation of GPS multipath and receiver tracking errors.  
*Navigation: Journal of the Institute of Navigation*, **41**, 4  
(Winter 1994–1995), 415–434.
- [2] Braasch, M. (1997)  
Autocorrelation sidelobe considerations in the  
characterization of multipath errors.  
*IEEE Transactions on Aerospace and Electronic Systems*,  
**33**, 1 (Jan. 1997), 290–295.
- [3] Townsend, B., et al. (1995)  
Performance evaluation of the multipath estimating delay  
lock loop.  
*Navigation: Journal of the Institute of Navigation*, **42**, 3  
(Fall 1995), 503–514.
- [4] Tomita, H. (1974)  
Experiments on the effects of multipath signals for a  
non-coherent delay lock receiver.  
Report TOR-0074(4461-03)-5, Systems Engineering  
Operations, The Aerospace Corporation, Mar. 29, 1974.
- [5] Van Nee, R. (1995)  
Multipath and multi-transmitter interference in  
spread-spectrum communication and navigation systems.  
Ph.D. dissertation, Delft University of Technology, Delft,  
The Netherlands, 1995.
- [6] Braasch, M. (1996)  
Multipath effects.  
*Global Positioning System: Theory and Applications*, Vol.  
I, American Institute of Aeronautics and Astronautics,  
Washington, D.C., ch. 14.
- [7] Van Dierendonck, A., et al. (1992)  
Theory and performance of narrow correlator spacing in a  
GPS receiver.  
*Navigation: Journal of the Institute of Navigation*, **39**, 3  
(Fall 1992), 265–283.
- [8] Braasch, M., and Van Dierendonck, A. (1999)  
GPS receiver architectures and measurements.  
*Proceedings of the IEEE*, **87**, 1 (Jan. 1999), 48–64.
- [9] Macabiau, C., Roturier, B., Chatre, E., and Yazid, R. (2000)  
*N*-multipath performance of GPS receivers.  
*In Proceedings of the IEEE Position, Location and  
Navigation Symposium (PLANS 2000)*, San Diego, CA,  
Mar. 13–16, 2000, 41–48.
- [10] Cox, D., Shallberg, K., and Manz, A. (1999)  
Definition and analysis of WAAS receiver multipath error  
envelopes.  
*In Proceedings of the 1999 National Technical Meeting of  
the Institute of Navigation*, San Diego, CA, Jan. 25–29,  
1999, 827–838.

## Acoustic Hit Indicator

**An improved acoustic target is considered. Acoustic targets estimate the hit coordinates of a supersonic projectile using the time of arrival (TOA) of the supersonic shock wave at several acoustic transducers located in the vicinity of the target. An improved target allows oblique hits, likely in firing practices involving roaming infantry and armor. Four trajectory parameters are estimated: two hit coordinates ( $x, h$ ) on a virtual, vertical, target plane; horizontal angle of incidence; projectile velocity. Explicit expressions are provided of the expected TOA measurements and their derivatives with respect to the estimated parameters. The expressions simplify a least-squares iterative algorithm and accelerate its convergence. Expected error contour maps are provided.**

### I. INTRODUCTION

The sharp rise-time of the pressure shock, created by the passage of a supersonic projectile [1–3], enables an accurate measurement of its time of arrival (TOA). The TOA of the shock at various transducer locations can yield information on the projectile trajectory, in particular where it hits a target plane. Among the advantages of an acoustic target relative to a solid target silhouette are freedom from patching old hit marks, and the ability to indicate miss coordinates outside the silhouette. The subject of measuring an acoustic shock wave and its TOA is well covered in scientific journals [2, 3]. On the other hand, the literature on utilizing these acoustic measurements to estimate the projectile trajectory is constituted almost entirely of patent disclosures. It is time to introduce this interesting topic into the scientific literature as well.

Existing acoustic targets, found in firing ranges for target practice, can be divided into two categories. 1) Targets whose front is a thin acoustic chamber [4], with face wall made of rubber membrane. The acoustic transducers are located within the chamber and detect disturbances created by the bullet while passing through the chamber and are guided within the chamber. 2) Open-air targets, in which the acoustic disturbance is not guided. Open-air targets are usually restricted to perpendicular hits, and utilize very specific transducer locations (e.g., arranged in

Manuscript received November 5, 1999; revised June 19 and  
October 24, 2000; released for publication November 20, 2000.

IEEE Log No. T-AES/37/1/02940.

Refereeing of this contribution was handled by J. P. Y. Lee.

0018-9251/01/\$10.00 © 2001 IEEE

two triangular array [5]). With these constraints it was possible to find an algebraic solution of the hit coordinates. On the other hand, Bowyer, et al. [6] describe a general approach that makes almost no assumptions about the trajectory. Bowyer's approach permits both horizontal and vertical components of the angle of incidence, air drag, and three components of the wind vector. In order to estimate the additional parameters, additional transducers are required and only an iterative solution is practical. Bowyer's patent contains a single implicit vector equation in which both the measurements and the parameters are inseparably embedded.

We deal here with large open-air targets. We show that few practical assumptions about the trajectory make it possible to express each individual TOA measurement as an explicit function of the estimated parameters and of the three coordinates of the corresponding transducer. We also present the partial derivatives of the expected measurement with respect to the estimated parameters. Explicit expressions of the measurements and their derivatives simplify the iterative algorithm (e.g., Gauss-Newton) and improve its convergence rate.

Three assumptions are made about the trajectory: 1) negligible vertical incidence angle, 2) constant projectile velocity (in the vicinity of the target), and 3) negligible wind. Assumptions 1 and 2 are practical for most direct-fire cases. Assumption 3 is not always true. Strong winds may induce bias errors. However, in most cases the bias error caused by ignoring wind are likely to be smaller than the increase in random error when additional wind components are added to the list of estimated parameters.

The main contribution of this work is the mathematical handling of *oblique* hits. Allowing and estimating a horizontal incidence angle is very important. Modern firing practices involve roaming infantry and armor, and pop-up targets that will not always face the fire source. Horizontal incidence angle of up to  $45^\circ$  can be expected. The ability to estimate the incidence angle enables an acoustic array to also determine the direction of hostile direct-fire. This is an important application by itself. Furthermore, the combination of incidence angle and estimated projectile terminal velocity can yield a coarse estimate of the location of the fire source.

Prototypes of the acoustic hit indicator were built and tested successfully with both rifle bullets and tank rounds. A U.S. Patent [7] was granted.

In the remaining sections the TOA equations and their derivatives are derived. The iterative algorithm is outlined, and the theoretical error expressions are given. Finally, for one example of transducer arrangement, the distribution of the expected position, angle, and velocity estimation error, over the target plan, is presented in a set of contour maps.

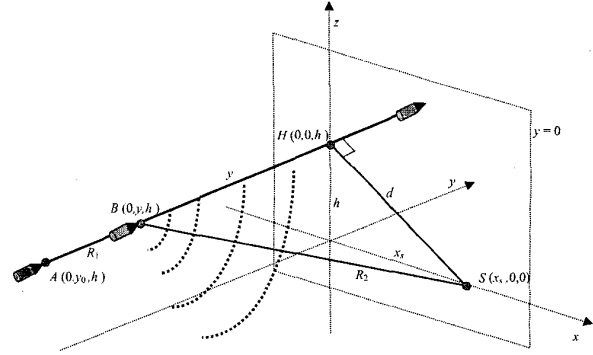


Fig. 1. Geometry of perpendicular hit.

## II. TOA EQUATIONS FOR A PERPENDICULAR HIT

While the main contribution of this work is the shock wave time of arrival (TOA) equation for an *oblique* hit (see (9)), we first develop the TOA equation for the simpler case of a *perpendicular* hit (Fig. 1). The virtual target plane is the  $y = 0$  plane. The supersonic projectile travels along the line defined by  $x = 0$ ,  $z = h$ , and intersects the target plane at point  $H(0,0,h)$ . A transducer  $S(x_s, 0, 0)$  is located on the target plane (not a requirement). Let the time origin  $t = 0$  be defined as the epoch when the projectile passed through an arbitrary point  $A(0, y_0, h)$ , located early enough along the trajectory. The projectile  $B$  generates pressure disturbances all along its travel. These disturbances are detected by transducer  $S$ . Because the projectile velocity is higher than the speed of sound, the disturbances are detected at  $S$  not in the order in which they were generated. The disturbance from one special point  $B_f$  will be the first to reach transducer  $S$ . By definition its arrival matches the detection of the shock wave by transducer  $S$ . Fig. 1 and the following discussion help us find point  $B_f$  and from it the arrival time of the shock wave.

A pressure disturbance generated by the projectile when it passes through an arbitrary point  $B$ , is sensed by transducer  $S$  at a time  $t_s$  (measured from when the projectile crossed point  $A$ ). The time duration  $t_s$  is the sum of two time durations. The first one is the time it takes the projectile to travel distance  $R_1$  from point  $A$  to point  $B(0, y, h)$ , at the projectile velocity  $V$ . The second one is the time it takes the sound to travel distance  $R_2$  from point  $B$  to transducer  $S$ , at the speed of sound  $C$ , hence

$$t_s = \frac{R_1}{V} + \frac{R_2}{C} = \frac{y - y_0}{V} + \frac{\sqrt{y^2 + d^2}}{C} \quad (1)$$

where

$$d = \sqrt{x_s^2 + h^2} \quad (2)$$

and  $y$  is the distance of the corresponding point  $B$  from the target plane (in Fig. 1  $y < 0$ ).

To find the location of  $B_f(0, y_f, h)$ , we find the shortest  $t_s$  by taking the derivative of (1) with respect

to  $y$ , and marking the resulting  $y$  as  $y_f$

$$\left. \frac{\partial t_s}{\partial y} \right|_{y=y_f} = 0. \quad (3)$$

Again, the physical meaning of  $y_f$  is the location of the projectile along its trajectory, from where the pressure disturbance was the first to arrive at the transducer. Performing (3) yields

$$y_f = -\frac{d}{\sqrt{\frac{V^2}{C^2} - 1}}, \quad V > C. \quad (4)$$

It is interesting to find a typical  $y_f$ . Using the typical values  $d = 2$  m and  $V = 2C$  yields  $y_f = -1.15$  m. This result implies that the leading edge of the shock wave is likely to originate when the projectile is about 1 m in front of the target.

Substituting  $y_f$  instead of  $y$  in (1) yields the TOA of the shock wave at the transducer

$$t_{s,\min} = -\frac{y_0}{V} + d\sqrt{\frac{1}{C^2} - \frac{1}{V^2}}, \quad V > C. \quad (5)$$

For the general case when there are  $N$  transducers located at  $x_k, y_k, z_k, k = 1, 2, \dots, N$  and the hit coordinate is at  $(x, 0, h)$ , the TOA of the shock wave at the  $k$ th transducer is given by

$$t_k = -\frac{y_0}{V} + \frac{y_k}{V} + \sqrt{(x - x_k)^2 + (h - z_k)^2} \sqrt{\frac{1}{C^2} - \frac{1}{V^2}}, \quad k = 1, 2, \dots, N. \quad (6)$$

Note that the term  $-y_0/V$  is an arbitrary delay term common to all the transducers. It resulted from an arbitrary definition of the reference time  $t = 0$ , as the epoch when the projectile passed through the arbitrary point A. The reference time could be chosen at any other instance of time. Hence we can replace the term  $-y_0/V$  by a common time offset  $t_{\text{offset}}$ , and rewrite (6) as

$$t_k = t_{\text{offset}} + \frac{y_k}{V} + \sqrt{(x - x_k)^2 + (h - z_k)^2} \sqrt{\frac{1}{C^2} - \frac{1}{V^2}}, \quad k = 1, 2, \dots, N. \quad (7)$$

A practical choice of  $t_{\text{offset}}$  is the epoch at which the shock wave was first detected by one of the transducers.

Equation (7) contains 4 unknowns:  $x, h, V, t_{\text{offset}}$ . Hence, at least 4 transducers are required. The speed of sound  $C$  need not be included as an unknown.  $C$  in m/s can be derived from the prevailing air temperature  $T$  in deg Kelvin, using the well-known approximation [8]

$$C_{[\text{m/s}]} = 20.05\sqrt{T_{[\text{°K}]}}. \quad (8)$$

However,  $C$  can become an additional unknown, and solved simultaneously with the other four, if the number of transducers is at least five.

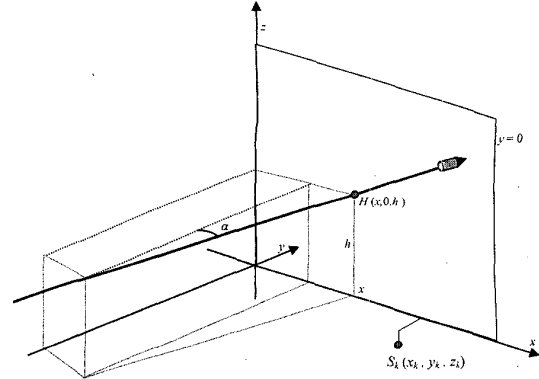


Fig. 2. Geometry of oblique hit.

### III. TOA EQUATIONS FOR AN OBLIQUE HIT

When the horizontal angle  $\alpha$  between the trajectory and the normal to the target plane is not necessarily zero (Fig. 2), the derivation of the TOA equation is more elaborate than the derivation which led to (7). The new TOA equations for the  $k = 1, 2, \dots, N$  sensors become

$$t_k = t_{\text{offset}} - \frac{1}{V} [(x - x_k) \sin \alpha - y_k \cos \alpha] + \sqrt{[(x - x_k) \cos \alpha + y_k \sin \alpha]^2 + (h - h_k)^2} \times \sqrt{\frac{1}{C^2} - \frac{1}{V^2}}. \quad (9)$$

Note that for  $\alpha = 0$ , (9) reduces to (7). It is important to realize that (9) is a prediction of the noise-free TOA measurement expected at the  $k$ th sensor if the hit coordinates are  $(x, h)$ , the projectile velocity is  $V$ , and the incidence angle is  $\alpha$ .

To the best of our knowledge such an explicit expression of the expected measurement of an acoustic shock wave TOA for an oblique hit was not derived before. Having such an explicit equation of the expected practical measurement, together with its derivatives (listed below), allows a very simple and quick iterative solution of the hit coordinates.

In order to implement an iterative Gauss-Newton algorithm, it is helpful to have explicit expressions of the partial derivatives of (9) with respect to each one of the estimated parameters. For convenience of notation let us first define

$$Q_k = \sqrt{[(x - x_k) \cos \alpha + y_k \sin \alpha]^2 + (h - h_k)^2}, \quad k = 1, 2, \dots, N. \quad (10)$$

From (9) and using (10) we obtain all the required derivatives:

$$\frac{\partial t_k}{\partial x} = -\frac{\sin \alpha}{V} + \frac{1}{Q_k} \sqrt{\frac{1}{C^2} - \frac{1}{V^2}} \times [(x - x_k) \cos \alpha + y_k \sin \alpha] \cos \alpha \quad (11)$$

$$\frac{\partial t_k}{\partial V} = \frac{1}{V^2}[(x - x_k)\sin\alpha - y_k\cos\alpha] + \frac{Q_k}{V^3\sqrt{\frac{1}{C^2} - \frac{1}{V^2}}} \quad (12)$$

$$\frac{\partial t_k}{\partial h} = \frac{h - z_k}{Q_k}\sqrt{\frac{1}{C^2} - \frac{1}{V^2}} \quad (13)$$

$$\frac{\partial t_k}{\partial \alpha} = -[(x - x_k)\cos\alpha + y_k\sin\alpha] \times \left\{ \frac{1}{V} + \frac{1}{Q_k}\sqrt{\frac{1}{C^2} - \frac{1}{V^2}}[(x - x_k)\sin\alpha - y_k\cos\alpha] \right\} \quad (14)$$

$$\frac{\partial t_k}{\partial t_{\text{offset}}} = 1 \quad (15)$$

$$\frac{\partial t_k}{\partial C} = -\frac{Q_k}{C^3\sqrt{\frac{1}{C^2} - \frac{1}{V^2}}} \quad (16)$$

The last derivative is needed only if the speed of sound  $C$  is estimated from the TOA measurements. The actual measurements, an initial guess of the trajectory parameters and (9)–(16), can now be used in an iterative Gauss–Newton algorithm to produce a least-squares estimate of the five parameters.

#### IV. ITERATIVE ALGORITHM

In order to simplify the notations we define our equations in matrix and vector forms. The vector of unknowns (assuming the speed of sound is known) is defined as

$$\mathbf{x} = [x \ h \ V \ \alpha \ t_{\text{offset}}]^T \quad (17)$$

where the superscript T represents the transpose operation. The vector of calculated TOA is defined using (9), as

$$\mathbf{M}(\mathbf{x}) = [t_1(\mathbf{x}) \ t_2(\mathbf{x}), \dots, t_N(\mathbf{x})]^T \quad (18)$$

The actual TOA measurements, are arranged in a corresponding vector  $\mathbf{M}_{\text{measured}}$ . The partial derivative matrix is an  $N \times 5$  matrix whose  $(k, j)$  element is defined as

$$\mathbf{H}(\mathbf{x})_{k,j} = \frac{\partial t_k}{\partial \mathbf{x}_j} \quad (19)$$

where  $\mathbf{x}_j$  is the  $j$ th element of the vector of unknowns, defined in (17).

A recommended initial guess of the iterative algorithm is  $t_{\text{offset}} = 0$ ,  $\alpha = 0$ ,  $x$  and  $h$  at the center of the target, and  $V$  the typical velocity of the projectile. The updated estimate following the  $i$ th iteration is

$$\mathbf{x}_{(i+1)} = \mathbf{x}_{(i)} + (\mathbf{H}^T\mathbf{H})^{-1}\mathbf{H}^T[\mathbf{M}_{\text{measured}} - \mathbf{M}(\mathbf{x}_{(i)})] \quad (20)$$

where the partial derivative matrix in (20) uses the last estimate of the unknowns, namely

$$\mathbf{H} = \mathbf{H}(\mathbf{x}_{(i)}) \quad (21)$$

The iteration process continues until the sum of squares of the changes in the values of  $\mathbf{x}$ , drops below a predetermined threshold. When the number of transducers is larger than the number of unknowns, the vector of residuals after the last iteration

$$\mathbf{R}_{(i)} = [\mathbf{M}_{\text{measured}} - \mathbf{M}(\mathbf{x}_{(i)})] \quad (22)$$

will not be identically zero. If one of its elements is considerably larger than the rest, it can be considered an outlier. In such a case it is better to ignore the corresponding measurement and repeat the iterative process with  $N - 1$  measurements. When a transducer repeatedly produces outliers it may be an indication of a defective device.

#### V. EXPECTED RANDOM ERROR

Random TOA measurement errors cause random errors in the estimated parameters. If the random errors in the TOA measurements are independent and identically distributed (IID) with a zero-mean Gaussian distribution having a standard deviation (STD)  $\sigma_t$ , then the random error in the  $j$ th estimated parameters will also be zero-mean Gaussian with STD given by

$$\sigma_{\mathbf{x}_j} = \sigma_t\sqrt{(\mathbf{H}^T\mathbf{H})_{j,j}^{-1}} \quad (23)$$

We are interested in the total hit position error, whose distribution is Rayleigh with an rms value given by

$$\sigma_p = \sqrt{\sigma_x^2 + \sigma_h^2} = \sigma_t\sqrt{(\mathbf{H}^T\mathbf{H})_{1,1}^{-1} + (\mathbf{H}^T\mathbf{H})_{2,2}^{-1}} \quad (24)$$

in the incidence-angle error

$$\sigma_\alpha = \sigma_t\sqrt{(\mathbf{H}^T\mathbf{H})_{4,4}^{-1}} \quad (25)$$

and in the velocity error

$$\sigma_V = \sigma_t\sqrt{(\mathbf{H}^T\mathbf{H})_{3,3}^{-1}} \quad (26)$$

In Fig. 3 we present an example of a  $4 \times 2$  m target and a 7 transducer array. The transducer locations are listed in Table I. Such a large target (resembling a tank silhouette) is found in armor firing ranges, where oblique hits are very likely. The tank application also prompted locating the transducers below the silhouette, to reduce their chance of being hit.

Fig. 4 is a contour map of the resulting total hit position estimation error rms (see (24)) for that example. The TOA measurement error is assumed to be normally distributed with zero mean and the STD is  $\sigma_t = 10 \mu\text{s}$ . The projectile velocity is 800 m/s and the incidence angle is zero (both unknown to the estimator). The speed of sound was 345 m/s (known to the estimator). Fig. 4 shows that the position of a hit anywhere on the  $4 \times 2$  m target is estimated with rms error smaller than 4 cm.

TABLE I  
Transducer Location Relative to the Center of the Target Base

#	1	2	3	4	5	6	7
x [m]	-2.2	-2.2	-1.1	0	1.1	2.2	2.2
y [m]	-0.5	0	0	0	0	0	-0.5
z [m]	-0.5	-0.5	-0.5	-0.75	-0.5	-0.5	-0.5

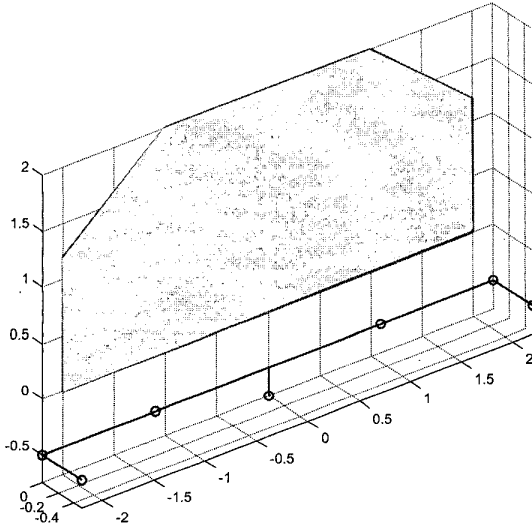


Fig. 3. Example of 4 × 2 m target and 7 transducer array.

Note that a TOA measurement error could be attributed to a combination of actual error in time measurement and to errors in the position of the transducers. A 10 μs TOA error corresponds roughly to a 0.34 cm transducer position error. Note also that while the silhouette in Fig. 3 is defined by  $-2 \leq x \leq 2$  m,  $y = 0$ ,  $0 \leq z \leq 2$  m, hits in the vicinity but outside the silhouette are also measured. For the given example the solved hit coordinates are given relative to point  $x = 0$ ,  $z = 0$  on the  $y = 0$  plane. In general the hit coordinates can be given relative to a translation or rotation of the coordinate system, as long as the transducer locations are also given in the new coordinates system. The role of the silhouette is to present the target to the marksman. In that respect, the location of a reference mark on the silhouette must be known in the same coordinate system, if scoring is based on how close the point of impact is to the mark.

Figs. 5 and 6 present the rms error of the estimated incidence angle and projectile velocity, respectively. Fig. 5 indicates rms error of 0.6° or less in the estimated incidence angle. Fig. 6 indicates rms error of 16 m/s or less in the estimated projectile velocity (out of a nominal value of 800 m/s). Both errors are linearly related to the delay measurement error rms, which was assumed as 10 μs.

Fig. 7 is a contour map of the resulting total hit position error rms when the incidence angle is

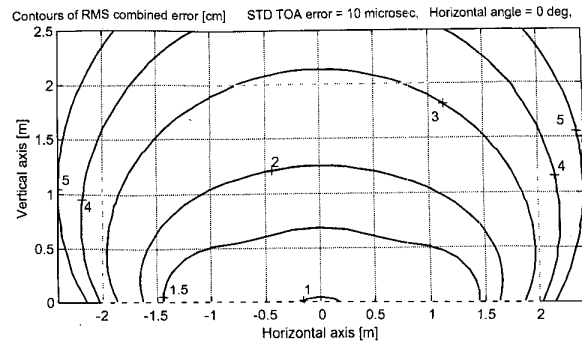


Fig. 4. Contours of expected total hit position rms error (in cm).

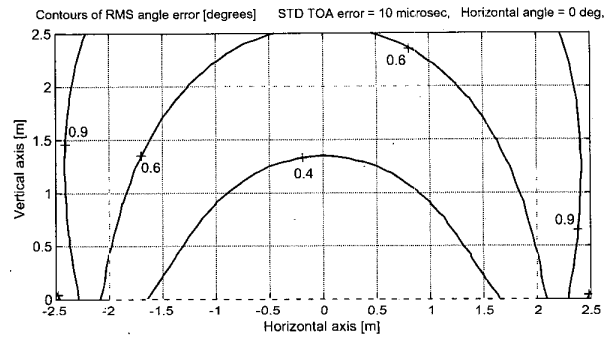


Fig. 5. Contours of expected incidence angle error STD (in degrees).

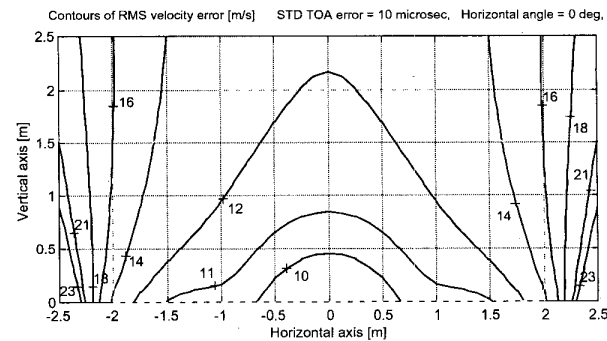


Fig. 6. Contours of expected velocity rms error (in m/s).  
Nominal velocity is 800 m/s.

$\alpha = 30^\circ$ . Comparing it with Fig. 4 ( $\alpha = 0^\circ$ ) shows only minor degradation.

Studies of error contour maps, for different transducer locations, indicate that it is advantageous to locate at least one transducer at a different

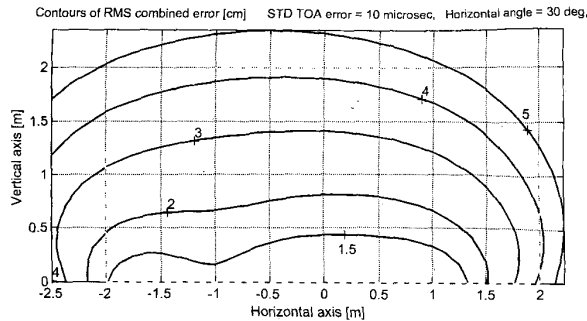


Fig. 7. Expected total hit position rms error contours (cm) when incidence angle is  $30^\circ$ .

horizontal distance from the target, than the rest of the transducers (1 and 7 in Table I). If the speed of sound is also estimated, it is advantageous to position at least one transducer below the rest (4 in Table I).

The linear dependence of the estimated error on the measurement error, shown in (24)–(26), implies that if the measurement error is different from the assumed  $\sigma_t = 10 \mu\text{s}$  by a factor, then the contour values in Figs. 4–7 will be multiplied by the same factor.

Contrary to intuition, geometrically scaling down the target and the array by a factor does not scale down the values of the hit error contours. For example, if the silhouette and the transducer array were reduced by a factor of 4, the hit position rms error contours will look exactly like Fig. 4, except that the horizontal and vertical scales will be smaller by a factor of 4. For example, the 3 cm error contour line will still follow closely the edge of the smaller ( $-0.5 \leq x \leq 0.5 \text{ m}$ ,  $0 \leq z \leq 0.5 \text{ m}$ ) silhouette, as it does in Fig. 4 for the original silhouette. Furthermore, the angle and velocity error contours will increase by that factor.

The means to reduce hit position errors in a small target are to improve the delay measurement error and the accuracy of the transducer location, and to spread the transducer array around the silhouette rather than below it. Furthermore, since small competition targets usually serve perpendicular firing, the angle of incidence could be treated as a known parameter. This will improve the estimation accuracy of the remaining parameters.

## VI. CONCLUSIONS

A practical algorithm was presented for determining the trajectory of a supersonic projectile intersecting a virtual target plane. The algorithm utilizes measurements of the TOA of the supersonic shock wave at a transducer array. The algorithm handles an important additional estimated parameter—a horizontal incidence angle. This feature allows coverage of nonperpendicular hits. Oblique

hits are likely to occur in modern armor and infantry training ranges. This feature could be used also to determine direction of hostile fire (counter-sniper). The main contribution of this work is an explicit equation of the measured TOA of the supersonic shock wave, for an oblique hit, as a function of the estimated parameters and the transducer coordinates (9). The TOA equation and its derivatives with respect to the estimated parameters (10)–(16) enable a simple and fast solution for the trajectory parameters using a Gauss–Newton least-squares iterative algorithm. The array requires at least 5 transducers. There are almost no restrictions on the transducer locations. The partial derivatives also enable predicting the expected accuracy of the estimated parameters for any given array.

NADAV LEVANON  
 Dept. of Electrical Engineering–Systems  
 Tel Aviv University  
 Tel Aviv, 69978  
 Israel

## REFERENCES

- [1] Raspet, R. (1997) Shock waves, blast wave, and sonic booms. In M. J. Crocker (Ed.), *Encyclopedia of Acoustics*. New York: Wiley, 1997, ch. 31.
- [2] Stoughton, R. (1997) Measurements of small-caliber ballistic shock waves in air. *Journal of the Acoustical Society of America*, **102** (Aug. 1997), 781–787.
- [3] Sadler, B. M., Pham, T., and Sadler, L. C. (1998) Optimal and wavelet-based shock wave detection and estimation. *Journal of the Acoustical Society of America*, **104** (Aug. 1998), 955–963.
- [4] Mobasser, B. G. (1995) Automatic target scoring system using machine vision. *Machine Vision and Applications*, **8** (Jan. 1995), 20–30.
- [5] McCarthy, B. D., and Regan, B. J. (1989) Position measuring apparatus and method. US Patent 4,885,725, issued Dec. 5, 1989.
- [6] Bowyer, W. H., and Newnham, R. (1981) Shock wave triggered target indicating system. US Patent 4,261,579, issued Apr. 14, 1981.
- [7] Levanon, N. (1999) Acoustic hit indicator. US Patent 5,920,522, issued July 6, 1999.
- [8] Wong, G. S. K., and Embleton, T. F. W. (1985) Variation of the speed of sound in air with humidity and temperature. *Journal of the Acoustical Society of America*, **77** (May 1985), 1710–1712.